516-34
185276

N94-12300

Progress in modeling hypersonic turbulent boundary layers

By O. Zeman

1. Motivations and objectives

A good knowledge of the turbulence structure, wall heat transfer, and friction in turbulent boundary layers (TBL) at high speeds is required for the design of hypersonic airbreathing airplanes and reentry space vehicles. This work reports on recent progress in modeling of high speed TBL flows. The specific research goal described here is the development of a second order closure model for zero pressure gradient TBL's for the range of Mach numbers up to hypersonic speeds with arbitrary wall cooling requirement.

2. Accomplishments

In this report, new compressible models and theories that lead to their development are reviewed with the focus on compressibility effects in quasi-equilibrium turbulent boundary layers. The primary purposes are to report on a new second order closure model (SOC) developed for hypersonic TBL's and to present comparison of model results with experiments in zero pressure gradient TBL's up to freestream Mach number $M_e = 10.3$. The following section is a modified and abbreviated version of the paper of Zeman (1993). The model described in subsection 2.2.2 is a new contribution.

2.1 Introduction

Recent renewed interest in high speed aerodynamics has led to new developments in theory, simulation, and modeling of compressible turbulence. Availability of direct numerical simulations (DNS) of basic homogeneous compressible flows has greatly facilitated the development of new models for compressible turbulent flows. In view of the recent DNS results and experiments, it now appears that in many flows of practical interest, the turbulence cannot be treated by the so-called anelastic models, where the variation of *averaged* density and pressure are accounted for but not their fluctuating fields. In the past three years, this realization has lead to development of a variety of new models which account for the effect of fluctuating divergence (dilatation) on turbulence. In this paper, we shall focus mainly on the compressibility effects pertaining to TBL's with zero pressure gradients (ZPG). The paper is organized as follows: in the following section, we present the background and review of the current representation of the dilatational terms in the modeling equations. The subsequent sections highlight the new SOC model for super/hypersonic TBL's, make comparisons with experiments, and conclude with a discussion of compressibility effects in high speed TBL's and their consequences for the turbulence models.

2.2 Background, review

As shown first in Zeman[1], the Favre-averaged energy governing equations for homogeneous compressible turbulence, in the absence of any forcing, can be written as

$$\frac{1}{2}\frac{Dq^2}{Dt} = -(\epsilon_s + \epsilon_d - \Pi_d) \tag{1}$$

$$\frac{D\widetilde{T}}{Dt} = (\epsilon_s + \epsilon_d - \Pi_d)c_p^{-1}, \tag{2}$$

where $q^2/2 = \widetilde{u_j u_j}/2$ is the turbulence kinetic energy and $c_p\widetilde{T}$ is the mean enthalpy (Favre and Reynolds averages are denoted by tilde and overbar, respectively) and $\epsilon_s = \nu\overline{\omega_j\omega_j}$ is the solenoidal dissipation associated solely with the enstrophy $\overline{\omega_j\omega_j}$ (of the solenoidal velocity field). The compressibility effects are contained in two terms labeled ϵ_d and Π_d. These are associated with the dilatational (or compressive) velocity field which has nonzero dilatation $u_{j,j}$ (denoted hereafter by θ). Thus, the dilatation dissipation $\epsilon_d = \frac{4}{3}\nu\overline{\theta^2}$ and $\Pi_d = \overline{p\theta}/\overline{\rho}$ is the pressure-dilatation correlation (per unit mass). The compressive and solenoidal fields are strictly separable only in homogeneous turbulent flows; in TBL's, the treatment of ϵ_d and ϵ_s as two distinct contributions to total dissipation is valid only approximately.

2.2.1 Dilatation dissipation

The need for a representation in turbulence models of dilatational dissipation ϵ_d associated with fluctuating Mach number has been now recognized by many authors (see e.g. Viegas and Rubesin 1991; Wilcox 1991). Computational results indicate that in TBL's over insulated walls for $M_e \leq 9$, the maximum values of M_t are below 0.3, and hence ϵ_d due to shocklet dissipation is insignificant. However, in hypersonic TBL's with increasing wall cooling, the sonic speed a near the wall decreases and the M_t levels grow larger. The shocklet dissipation then assumes a controlling role: it maintains M_t below a certain threshold level, which according to the computations is always below $M_t = 1$; we find this aspect of the dissipation physically appealing. The basic expression for the shocklet dissipation given in Zeman (1990) is

$$\epsilon_d \propto \frac{q^3}{\ell}F(M_t^*, K) \tag{3}$$

where ℓ is a suitably defined turbulence lengthscale and $F(M_t^*, K)$ is a function of the r.m.s. Mach number. M_t^* is related to the *principal* r.m.s. Mach number $M_t = q/\sqrt{\gamma R\widetilde{T}}$ through $M_t^* = \sqrt{\frac{2}{\gamma+1}}M_t$. The parameter K is the kurtosis of the fluctuating speed $\sqrt{u_j u_j}$ intended to characterize intermittency of a particular turbulent flow. The computed curves $F(M_t^*, K)$ vs M_t^* for different K have been given in Fig. 2 of Zeman (1990). It is of note that the dependence of ϵ_d on the specific heat ratio γ (through M_t^*) improves the correlation of mixing layer growth rate with M_c, when the layer streams are gases with different values of γ (Viegas and Rubesin 1991).

In modeling (3D) turbulence, the quantities q^3/ℓ and ϵ_s are considered interchangeable; however, it should be emphasized that (3) is valid also in 2D turbulence (DNS only) where typically $q^3/\ell >> \epsilon_s$. We also point out that no near-wall correction is necessary in the expression for ϵ_d since F approaches zero at a much faster rate than the turbulent Reynolds number R_t (defined hereafter as $R_t = q^4/9\epsilon_s\nu$). As in high speed mixing layers, $F(M_t^*, K)$ for TBL's is approximated by an exponential function

$$F(M_t^*, K)) = \frac{\epsilon_d}{\epsilon_s} = c_d(1 - \exp\{-(\frac{M_t^* - M_{to}}{\sigma_M})^2\}). \tag{4}$$

The parameters c_d, M_{to}, and σ_M are functions of the kurtosis K to approximate the shape of the F-curves for a specified K (see Zeman 1993 for details).

2.2.2 Pressure-dilatation correlation in ZPG TBL's

In inhomogeneous flows, nontrivial contributions to the pressure-dilatation term arise from the interaction between the mean density gradient $\nabla\overline{\rho}$ and fluctuating pressure field. The derivation of the density-gradient contribution $(\overline{p\theta})_\rho$ to the pressure dilatation has been presented in Zeman (1991, 1993). The form of the model for flat plate TBL's (ZPG) is

$$(\overline{p\theta})_\rho = \tau q^2 \widetilde{u_2^2}(\overline{\rho}_{,2})^2 \frac{1}{\overline{\rho}} \tag{5}$$

In the SOC model, the contribution (5) is indispensable for assuring a proper (Van Driest) scaling of mean and fluctuating velocities in the inertial sublayer as shown in Zeman (1991, 1993). However, in the presence of wall heat transfer (cooling), the model (5) has proved to be ineffective in enforcing the correct scaling, and it had to be modified (as discussed briefly at the end of the following section).

2.3 Closure of the compressible TBL equations

In the boundary-layer approximation, the principal equations governing the mean flow field are the mass, momentum, and enthalpy conservation Favre-averaged equations

$$\frac{D\overline{\rho}}{Dt} = 0 \tag{6}$$

$$\overline{\rho}\frac{D\widetilde{U}_i}{Dt} = -\overline{p}_{,i} - (\overline{\rho}\widetilde{u_i u_j} - 2\mu S_{ij}^*)_{,j} \tag{7}$$

$$\overline{\rho}\frac{D\widetilde{T}}{Dt} = -(\overline{\rho}\widetilde{T' u_j}(1 - F_p) - \kappa\widetilde{T}_{,j})_{,j} + \overline{\rho}(\epsilon_s + \epsilon_d - \Pi_d)c_p^{-1}, \tag{8}$$

and the density is obtained from the equation of state $\overline{\rho} = p_e/(R\widetilde{T} + \widetilde{u_2^2})$ where p_e is the freestream (constant) pressure. F_p in (8) denotes the ratio of pressure to enthalpy fluxes $F_p = \overline{pu_i}/(\overline{\rho}c_p\widetilde{T' u_i})$. In compressible TBL's, F_p is expected to be non zero, and Zeman (1993) proposed an expression

$$F_p = 0.3(1 - exp\{-(\frac{M_t}{0.4})^2\}). \tag{9}$$

The coefficient (0.3) in (9) was chosen to recover the correct adiabatic wall temperature for the range $0 < M_e < 11$. The small M_t limit, $F_p \to M_t^2$ is required by scaling arguments.

It is of interest to note that if the turbulent fluctuations follow an adiabatic relation $p \propto \frac{\gamma}{\gamma-1}T'$, then F_p would be unity, and no heat would be transferred by turbulence. In the presence of heat sources, the compressive turbulence field is ineffective in transferring heat since it is virtually adiabatic; hence, the heat is transferred by the solenoidal turbulence only. In this sense, $1 - F_p$ in (8) reflects the reduced mixing efficiency due to turbulence of acoustic origin.

The remaining quantities needed to close the mean momentum and enthalpy equations (7) and (8) are the Reynolds stresses $\widetilde{u_i u_j}$ and the heat fluxes $\widetilde{T'u_i}$. General conservation equations for these quantities are shown in Zeman (1993). These equations contain the following terms requiring closure: pressure gradient-velocity and pressure gradient-temperature correlations denoted respectively by Π_{ij} and Π_i, the triple-moment (transport) terms, the solenoidal dissipation ϵ_s, and the compressibility terms ϵ_d and $\Pi_d \equiv \overline{p\theta}/\overline{p}$.

The pressure and transport terms are modeled in the same manner as their incompressible (Reynolds averaged) counterparts and developed previously by Zeman and Jensen (1987) for atmospheric TBL's (rough walls) and by Zeman (1990) for free compressible flows. Zeman (1993) modified the rapid part of Π_{ij} to account for the Reynolds number effects near smooth walls. This has been accomplished by making the coefficients associated with rapid terms, functions of the Reynolds number R_t. For the asymptotically large values of R_t, the rapid term coefficients converge to the values for the rough wall TBL as discussed above.

The effect of the rapid pressure terms Π_i and Π_{ij} is best illustrated by writing closure equations for the shear stress $\widetilde{u_1 u_2}$ and heat flux $\widetilde{T'u_2}$ in 2D flat plate TBL. With x_1 in streamwise and x_2 in wall-normal direction, one obtains

$$\frac{D\widetilde{u_1 u_2}}{Dt} = -C_m \frac{\widetilde{u_1 u_2}}{\tau} - 0.4(\widetilde{u_2^2} - 5\Delta\alpha b_{11} q^2)\widetilde{U}_{1,2} + \quad T.T. \tag{10}$$

$$\frac{D\widetilde{T'u_2}}{Dt} = -C_\theta \frac{\widetilde{T'u_2}}{\tau} - (\widetilde{u_2^2} - 5\Delta\alpha b_{11} q^2)\widetilde{T}_{,2} + \quad T.T. \tag{11}$$

We can immediately see that apart from the transport terms ($T.T.$), (10) and (11) have a similar form which also suggests that $|T'| \propto |u_1|$. The similarity has been achieved by the novel formulation of the rapid part of Π_i. By neglecting the advection and transport terms, (10) and (11) reduce to algebraic relations $\widetilde{u_1 u_2} = -\nu_T U_{1,2}$, and $\widetilde{T'u_2} = -\alpha_T \widetilde{T}_{,2}$ with the eddy viscosity and diffusivity ν_T and α_T being proportional, i.e.

$$\nu_T \propto \alpha_T \propto \tau \widetilde{u_2^2}[1 - 5\Delta\alpha \frac{b_{11}}{b_{22} + 1/3}]. \tag{12}$$

Hence, in the algebraic approximation, the model yields a constant turbulent Prandtl number $Pr_t = \nu_T/\alpha_T$; the model constants were chosen so that $Pr_t = 0.9$, the value which is supported by the DNS data in a channel flow, and by experiments in TBL's. In (12), b_{ij} is the anisotropy tensor and $\Delta\alpha$ is a R_t-dependent coefficient in the rapid pressure model (described in Zeman 1993).

The model equation for ϵ_s has a conventional form independent of M_t, except for the wall treatment. The wall boundary value $\epsilon_s(y=0)$ is determined from the approximate integral balance of the kinetic energy equation

$$\int_0^\infty \{P_s - \epsilon_s - \epsilon_d + \Pi_d\}dy = 0$$

where mean convection is ignored and the no-slip condition has been used. Furthermore, to eliminate the unphysical wall singularity in the ϵ_s-equation and in the return-to-isotropy pressure terms (due to $\tau = q^2/\epsilon_s \to 0$), the minimum τ is set by the Kolmogorov time scale

$$\tau \geq 5\sqrt{\frac{\nu}{\epsilon_s}}, \tag{13}$$

as suggested by Durbin (1991).

2.3.1 Modification of $\overline{p\theta}$ in the presence of wall heat flux

As mentioned earlier, in the presence of wall heat transfer, the model $(\overline{p\theta})_\rho$ in (5) has to be modified since the wall heat flux induces an entropic temperature field, giving spurious contributions to $\overline{p\theta}_\rho$. Zeman (1993) proposed to decompose the temperature field on the adiabatic contributions $T_a(\mathbf{x},t)$ (corresponding to an insulated wall TBL) and on the entropic contributions $T_s(\mathbf{x},t)$ which arise due to the surface heat flux alone (no dynamic heating); the actual temperature field is the sum $T = T_s + T_a$. The appropriate density gradient to be applied in (5) must be based on T_a, i.e. $\overline{\rho}_{,2}/\overline{\rho} \approx -(\widetilde{T}_a)_{,2}/\widetilde{T}$. The details of the determination of the entropic and adiabatic temperatures are presented in Zeman (1993).

2.4 Comparison with boundary layer experiments

The TBL computations are made by forward integration of the model equations starting with some initially thin TBL with the momentum thickness Reynolds number $Re_\theta = U_e\theta/\nu_e = 200-500$. The numerical scheme utilizes the compressible von Mises' transformation (Liepmann & Roshko 1967) in the inertial and outer region of the TBL where $y^+ \geq 30$, and, in the region below $y^+ = 30$ (where advection terms are negligible), the TBL is solved as a parallel flow. The vertical velocity in this region is nonzero (due to density variation) and is eliminated by the transformation to $\eta = \int_0^y \overline{\rho}/\rho_w dy$. This computational method is effective and accurate.

Fig. 1 is a sample of the model-experiment comparison: the streamwise r.m.s. fluctuations are plotted in a similarity form $(\overline{\rho}\widetilde{u_1^2}/\tau_w)^{1/2}$ vs. y/δ for a variety of Mach numbers and cooling rates. The universal behavior of the computed profiles is quite surprising; the cross-hatched area represents the measurements as compiled by Dussauge and Gaviglio (1987) (the first of these authors has pointed out to me that the low hot-wire value of u-fluctuations near the wall are likely due to errors associated with the transonic flow regime).

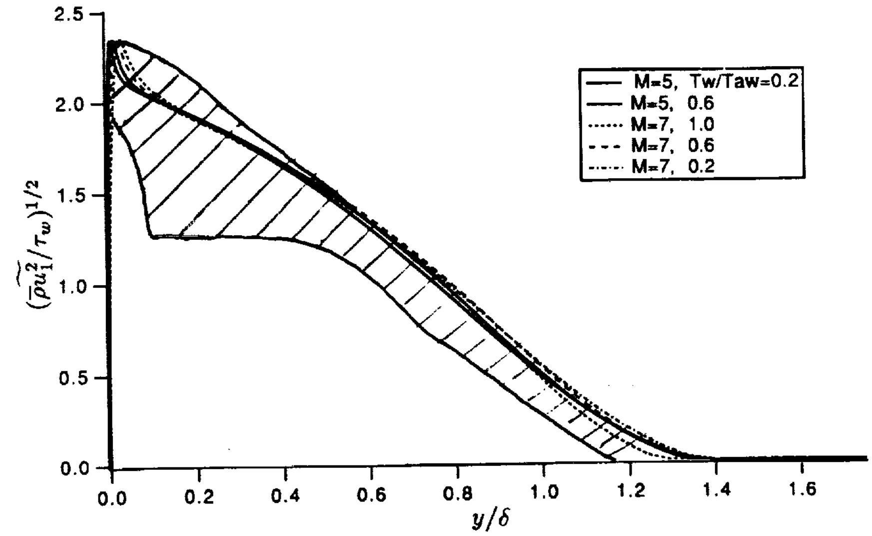

FIGURE 1. Similarity profiles of the streamwise r.m.s. fluctuations; cross-hatched area represents the scatter of experimental data compiled by Dussauge and Gaviglio (1986).

From a practical viewpoint, the most important test of a TBL model is its capability to predict the friction coefficient C_f and the Stanton number St, defined as

$$C_f = 2\frac{\tau_w}{\rho_e U_e^2} \quad St = \frac{q_w}{c_p \rho_e U_e (T_w - T_{aw})},$$

where q_w is the wall heat flux and T_{aw}, T_w are the adiabatic recovery and actual wall temperatures.

Fig. 2 shows standard plots of the ratio C_f/C_{fo} as a function of M_e and T_w/T_{aw} where C_{fo} is the low-speed value of $C_f(M_e \approx 0)$ corresponding to the same Re_θ. Fig. 2a shows the model-computed values of C_f/C_{fo} *vs* M_e, for an insulated-wall TBL for $Re_\theta \approx 10^4$ and the Van-Driest II curve; a few data points are shown in the hypersonic range. Fig. 2b shows C_f/C_{fo} *vs* T_w/T_{aw} for different M_e. The unknown value of C_{fo} is assumed $C_{fo} = 0.02632 Re_\theta^{-0.25}$. The model-computed values of C_f are in good agreement with theory and the data.

The model-experiment comparisons of St *vs* C_f is shown in Fig. 3. The model values (for the range $T_w/T_{aw} = 0.2 - 0.6$) indicate the Reynolds analogy factor $F_R = 2St/C_f \approx 1.2$; the displayed experimental values are in the range $F_R = 0.9 - 1.2$. In his review of experiments, Bradshaw (1977) suggests F_R be in the range $1.1 - 1.2$. In view of the likely experimental errors, the model predictions of the principal parameters C_f and St are consistent with the data and theory.

Fig. 4 consists of examples of the temperature profiles in the hypersonic range of Mach numbers. Fig. 4a shows model-experiment comparison of $\widetilde{T}/T_e(y/\delta)$ for an insulated-wall TBL in helium with $M_e = 10.3$; Fig. 4b is for $M = 8.2$ in air and with significant wall cooling ($T_w/T_{aw} = 0.28$). The computed temperature

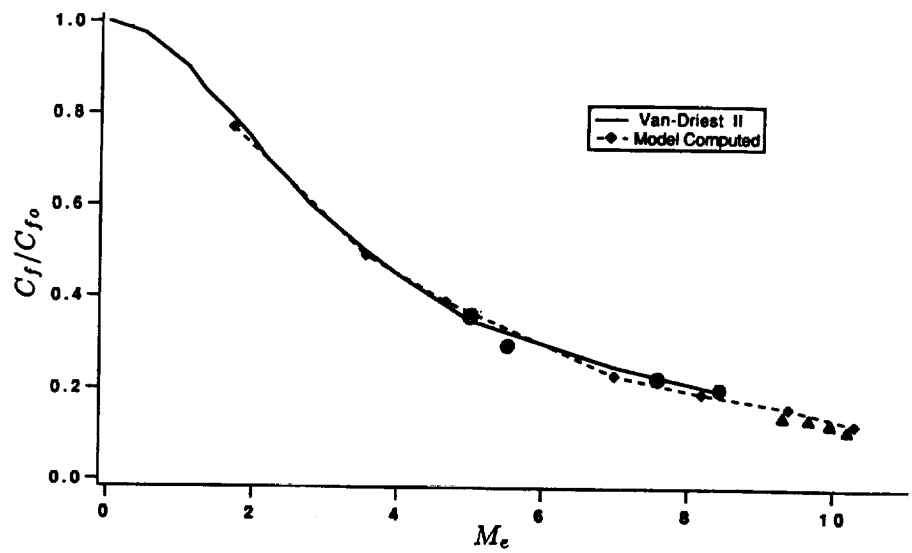

FIGURE 2. Variation of friction coefficient C_f/C_{f_o} vs. M_e at $R_\theta \approx 10^4$. Solid line is the Van-Driest II, data points labeled ▲ are from Watson (1978), and • are from Lobb *et al.* (shown in Liepmann and Roshko (1967).

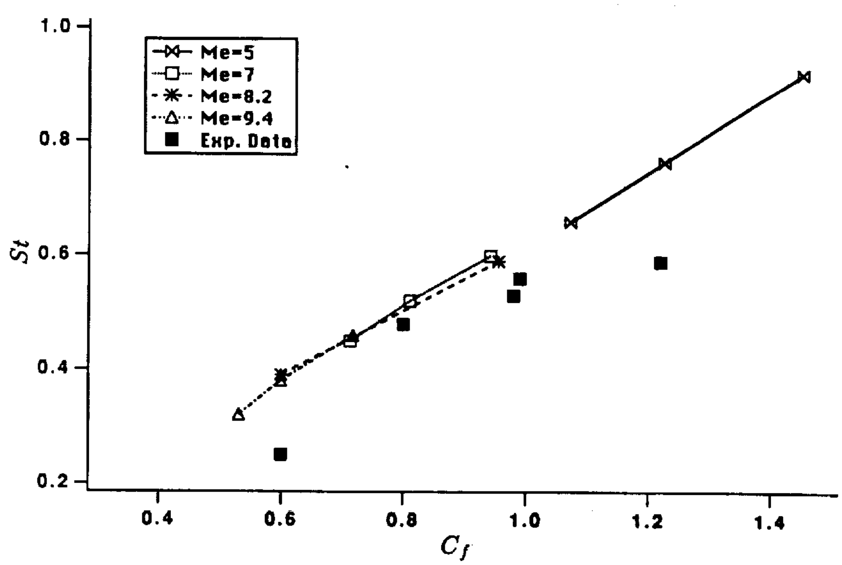

FIGURE 3. Variation of Stanton number St with C_f for $T_w/T_{aw} = 0.2 - 0.6$. Experimental data are from Laderman and Demetriades (1974), Kussoy and Horstman (1992), and Marvin and Coakley (1989).

profiles compare well with experiments (conducted on a sharp-edge flat plate). Of particular note is the prediction of the recovery temperature in the adiabatic TBL and of the temperature maximum near the wall in the cooled TBL.

To demonstrate the model performance at low speeds, in Fig. 5 the modeled velocity profile $U^+(y^+)$ is compared with the DNS results of Spalart (1988). Although Spalart's TBL Reynolds number, $Re_\theta = 1410$, is below what is considered a minimum self-similarity value, $Re_\theta = 3000$, the model prediction is evidently in good agreement with the DNS.

2.5 Model transition-to-turbulence prediction

There are two kinds of transition to turbulence, what F. T. Smith calls the civilized and the savage. In the civilized transition, small disturbances grow in accordance with the appropriate instability mechanisms, eventually reaching a point where transition to turbulence is initiated by strong nonlinearities and formation of turbulent spots in the flow. In the savage, or by-pass transition, the stage of the orderly disturbance growth is bypassed, and turbulence is directly initiated by a nonlinear process.

A fair indicator of the tendency to transition is the momentum Reynolds number Re_θ of the pre-transition, laminar boundary layer. Re_θ accounts for the flow history, and the transition Reynolds number $Re_{\theta t}$ correlates well with the transition onset on flat plates. Typically, turbulence models use transition formulas which inform the model, on the basis of values of Re_θ, pressure gradient, and freestream turbulence intensity, when to turn on the eddy viscosity. Wilcox (1992) mentions the remarkable property of his k-ω model "to describe the nonlinear growth of flow instabilities from laminar flow into the turbulent flow regime." In order to recover the appropriate transition Reynolds number for the Blasius profile, Wilcox modified the model parameters (as functions of turbulent Reynolds number R_t). Hence again, a correction has been provided to inform the model when to begin to amplify turbulence.

A remarkable property of the present model is its capability to mimic transition without any specific corrections added. This capability was tested only for high Mach numbers, and the results for two freestream Mach numbers are depicted in Fig. 6. The computations started with a thin TBL with a relatively small $Re_\theta \leq 200$. As seen in Fig. 6, the turbulence is initially attenuated and the TBL laminarizes. Only when Re_θ reached a certain (transition) value do the residual fluctuations within the boundary layer begin to rapidly grow until an equilibrium TBL is attained. More detailed investigations showed that $(Re_\theta)_t$ increased with M_e in a manner reminiscent of observed experimental transition (assuming $(Re_\theta)_t \propto \sqrt{Re_x t}$).

It is of note that the transitional growth of turbulent energy first occurred in the upper part of the layer in the vicinity of the maximum of the mass vorticity $\bar{\rho}U_{,y}$ (generalized inflection point). It is known from the stability theory that $(\bar{\rho}U_{,y})_{max}$ is potentially a point of maximum instability growth. In the model, the coincidence between the maxima of q^2 and $\bar{\rho}U_{,y}$ is a combined effect of the pressure-dilatation term $\overline{p\theta}$ in (5) and of strong viscous damping near the wall. At $M_e \geq 5$, the

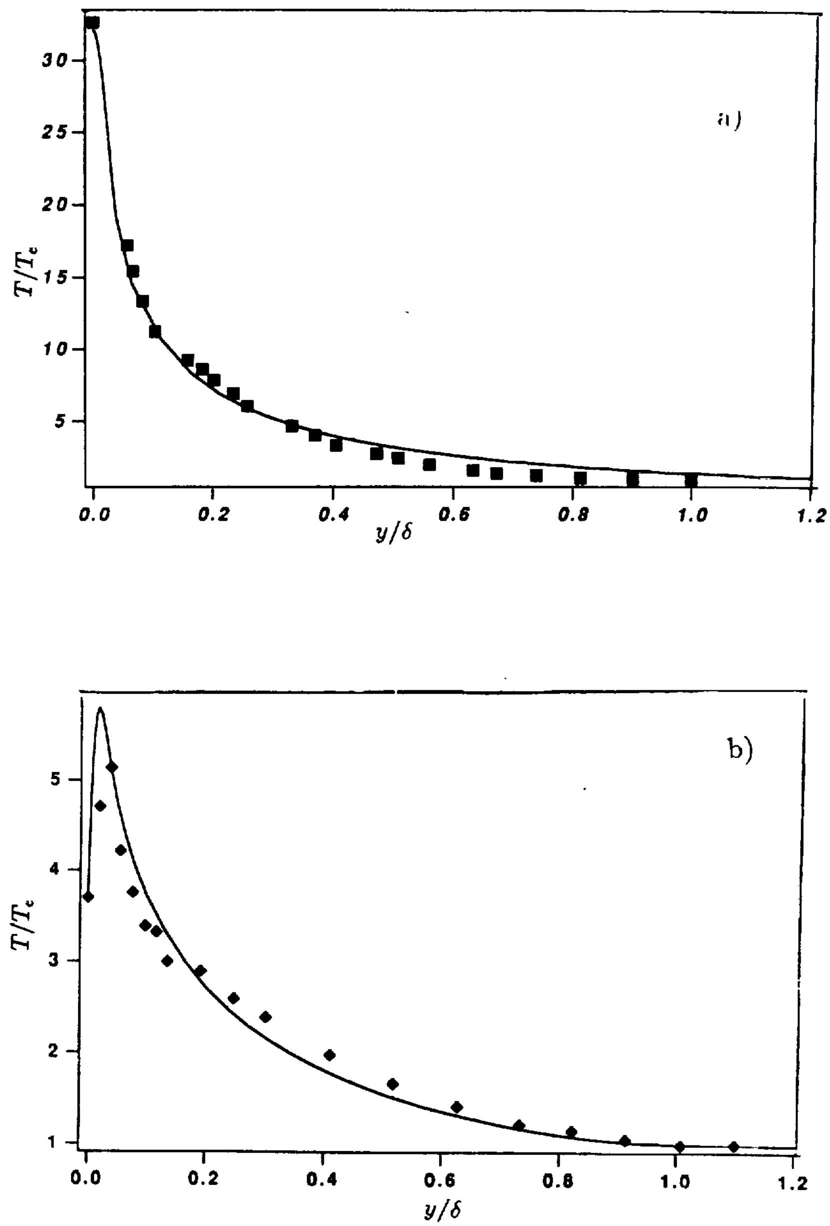

FIGURE 4 A& B. Model-experiment comparison of temperature profiles: a) data of Watson et. al. compiled in Fernholz and Finley (1977) under no. 73050504; $M_e = 10.31$, $R_\theta = 1.5 \times 10^4$, in helium. b) data from Kussoy and Horstman (1992) with $M_e = 8.2$, $T_w/T_{wa} = 0.28$, $R_\theta = 4.6 \times 10^3$.

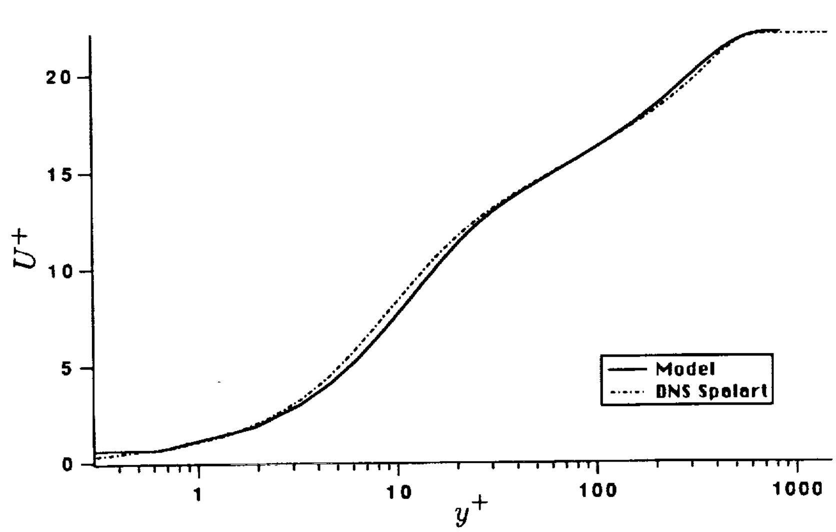

FIGURE 5. Model-DNS comparison of the velocity profiles $U^+(y^+)$. The DNS data are from Spalart (1988).

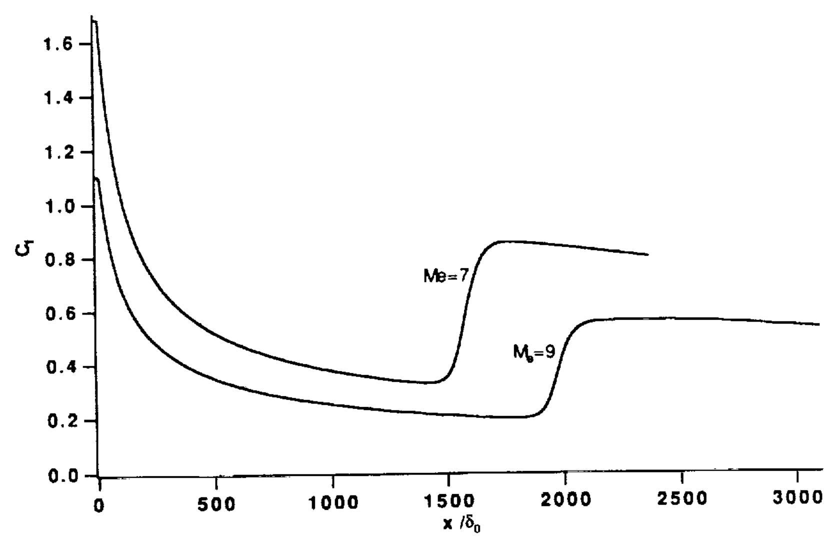

FIGURE 6. Laminarization and transition of a boundary layer at two different Mach numbers: SOC model results. The transition R_θ values are: for $M_e = 7$, $R_{\theta t} = 1100$; for $M_e = 9$, $R_{\theta t} = 1700$

incipient maximum production of q^2 is always in the upper part of the layer near the generalized inflection point; after the transition, the point of maximum q^2 moves towards the wall.

2.6 Discussion, Conclusions

We have developed a new SOC model intended for general applications in high-speed turbulent flows. It incorporates the latest advances in compressible turbulence theories and modeling. The explicit compressibility effect on turbulence is represented by models for the dilatation dissipation ϵ_d and pressure dilatation term $\overline{p\theta}$. Both ϵ_d and $\overline{p\theta}$ depend on the r.m.s. Mach number (M_t) and other structural parameters of the mean and fluctuating flow fields but not on the mean flow Mach number. The model predictions compare well with experiments for a wide range of Mach and Reynolds numbers. The importance of their contributions vary depending on flow speed and configuration.

In some recently published work, the importance of explicit compressibility corrections in TBL models has been questioned. It is indeed possible to adjust incompressible models to perform well in compressible regime without compressibility terms. However, ours is a more fundamental question: are the compressibility effects significant in reality, and can they be isolated in experiments and verified? If we consider DNS "experiments", then the answer is obviously yes. Both the dilatation dissipation and pressure dilatation terms have been identified in DNS of shear-generated and rapidly compressed turbulence. Their seeming unimportance in TBL's is only a question of degree. We find that as M_e and wall cooling increases, ϵ_d becomes increasingly important. In the hypersonic regime with $M_e > 7$ and sufficiently strong wall cooling, the standard k-ϵ models (without some form of dilatation dissipation) are likely to yield supersonic r.m.s. Mach number $M_t > 1$. This is obviously unrealistic; experimental evidence and DNS results suggest that M_t saturates well below unity.

Concerning the importance of the pressure dilatation $\overline{p\theta}$: the density-gradient contribution to $\overline{p\theta}$ constitutes a localized turbulence energy source which preserves the proper Van Driest scaling in the modeled TBL. The present results also suggest that $\overline{p\theta}$ counteracts the damping, viscous effects which have a tendency to laminarize the boundary layer at high values of M_e. The $\overline{p\theta}$-contributions are also related to the ability of the SOC model to mimic transition to turbulence. We intend to address these matters and the plausibility of modeling transitional (high-speed) flows in future investigations.

3. Future work

We shall continue to refine the new SOC model and search out more data for model-experiment comparison. We also hope to apply the model in nonequilibrium situations such as a compression corner flow.

In view of the ability of the SOC model to mimic transition, we shall attempt to investigate the connection between stability theory and model physics and to explore the potential of the SOC models to handle laminar and transitional regimes.

A major effort is going to be directed towards modeling nonequilibrium (incompressible) turbulence, such as in separated flows.

REFERENCES

BLAISDELL, G. A., MANSOUR, N. N.,& REYNOLDS, W.C. 1991 Numerical simulations of compressible homogeneous turbulence. *Ph. D. Thesis.* Mechanical Engineering Dept., Stanford University.

BLAISDELL, G. A. & ZEMAN, O. 1992 Investigation of the dilatation dissipation in compressible homogeneous shear flow. *Proceedings of the 1992 CTR Summer Program.* Stanford Univ./NASA Ames.

BRADSHAW, P. 1977 Compressible turbulent shear layers. *Annual Rev. Fluid Mech.* **9,** 33-54.

DURBIN, P. 1991 Near-wall turbulence closure modeling without "damping functions". *Theoret. Comput. Fluid Dyn.* **3,** 1-13.

FERNHOLZ, H. H., & FINLEY, P. J. 1977 A critical compilation of compressible turbulent boundary layer data. *AGARDograph No. 223.*

DUSSAUGE, J. P. & GAVIGLIO, J. 1987 The rapid expansion of a supersonic turbulent flow: the role of bulk dilatation. *J. Fluid Mech.* **174,** 81.

HORSTMAN, C. C. & OWEN, F. K. 1972 Turbulent properties of a compressible boundary layer. *AIAA J.* **10,** 1418.

KUSSOY, M. I. & HORSTMAN, K. C. 1992 Intersecting shock-wave/turbulent boundary layer interactions at Mach 8.3. *NASA Tech Memo 103909.*

LADERMAN, A. L. & DEMETRIADES, A. 1974 Mean and fluctuating flow measurements in the hypersonic boundary layer over a cooled wall. *J. Fluid Mech.* **63,** 121.

LIEPMANN, H. W. & ROSHKO, A. 1967 *Elements of Gas Dynamics.* John Wiley & Sons, pp 439.

MARVIN, J. G & COAKLEY, T. J. 1989 Turbulence modeling for hypersonic flows. 2nd Joint Europe/US Course in Hypersonics, 1989.

SARKAR, S., ERLEBACHER, G., HUSSAINI, M. Y. & KREISS, H. O. 1991 The analysis and modeling of dilatational terms in compressible turbulence. *J. Fluid Mech.* **227,** 473.

SPALART, P. R. 1988 Direct simulation of a turbulent boundary layer up to $R_\theta =$ 1410. *J. Fluid Mech.* **187,** 61-98.

VIEGAS, J. R., & RUBESI, M. W. 1991 A comparative study of several compressible models applied to high speed shear layers. AIAA paper 91-1783, June 1991, Honolulu, Hawaii.

WILCOX, D. C. 1991 Progress in hypersonic turbulence modeling. AIAA Paper 91-1785, 22nd Fluid Dynamics Conference, Honolulu, Hawaii.

WILCOX, D. C. 1992 The remarkable ability of turbulence model equations to describe transition. 5th Symposium on Numerical and Physical Aspects of Aerodynamic Flows, Long Beach, Florida, Jan. 1992.

WATSON, R. D. 1978 Characteristic of Mach 10 transitional and turbulent boundary layer. NASA Tech Paper 1243.

ZEMAN, O., & JENSEN, N. O. 1987 Modification of turbulence characteristics in flows over hills. *Q. J. Roy. Meteorol. Soc.* **113**, 5.

ZEMAN, O. 1990 Dilatation dissipation: The concept and application in modeling compressible mixing layers. *Phys. Fluids.* **A 2**, 178.

ZEMAN, O. 1991 The role of pressure-dilatation correlation in rapidly compressed turbulence. *CTR Annual Research Briefs 1991.* Stanford University/NASA Ames, 105-117.

ZEMAN, O. 1993 A new model for super/hypersonic turbulent boundary layers. *AIAA Paper 93-0897.* 31st Aerospace Science Meeting, Reno, Nevada, Jan. 1993.